2022

Application of metastable curve and crystal anisotropic for understanding tablet performance of pharmaceutical materials

Vivek Dhirubhai Patel
Long Island University

Arnold & Marie Schwartz College of Pharmacy and Health Sciences
Division of Pharmaceutical Sciences
Long Island University, Brooklyn, New York

Approval of the Ph.D. Dissertation

Application of metastable curve and crystal anisotropic for understanding tablet performance of pharmaceutical materials

Vivek D. Patel

Area of Specialization: Pharmaceutics

June 27th, 2022

Sponsoring Committee

_____

Rutesh H. Dave, Ph.D., Committee Chair

_____

Rahul V. Haware, Ph.D., Committee member

_____

Almas Babar, Ph.D., Committee member

_____

Qing Cai, Ph.D., Committee member

_____

Devang Patel, Ph.D., Committee member

_____ _____

Anthony J. Cutie, Ph.D.,
Division Chair

Christopher K. Surratt., Ph.D.
Associate Dean

Acknowledgements

It is my pleasure to acknowledge the roles of several individuals who played an important role for completion of my master research.

Firstly, I would like to express my gratitude to my mentor Dr. Rahul Haware for all his dedication and keen interest above all his overwhelming attitude to help his students had been solely and mainly responsible for completion my work. His timely advice, meticulous scrutiny, scholarly advice and scientific approach have helped me to very great extent to accomplish this task.

His valuable and keen supervision, incredible motivation, proper guidance, forbearance, and positive attitude inspirited me to achieve my goal.

I would also like to thank Dr. Dave, Dr. Morris, and Robert Sedlock for their permission to perform the experiments in their respective laboratories which helped to complete my project.

I am thankful to Savan Patel, Mitesh Kalathiya, Pathik Bavadiya, Yash Raichura, Jaydev Sonani, and Harsh Patel for remaining interested, supportive, and for giving me many things to enjoy outside of the Thesis project.

I thank my fellow lab mates Vishal Rathod, Harsh Shah4, Bhavin Parikh, Rusha Shardhara, Jayshil Bhatt, and Anusha for the stimulating discussions and all the fun during late night lab works.

I owe a special debt to my inspiration and would like to thank Munjal Patel, Urmil Bhatt, Raju Shah, Tejas Ruparelia, Parimal Patel, Chagan Lunagariya, Divyang Dave, and Yogi Chavada and their family for their moral support and helping me throughout the curriculum of my masters.

Finally, my deep and sincere gratitude to my family for their continuous and unparalleled love, help, and support. I am extremely grateful to my parents for their love, prayers, caring and sacrifices for educating and preparing me for my future. This journey would not be possible without them, and I dedicate this milestone to them.

I would like to dedicate this project to my father Dhiraj Patel, my mother Jayshree Patel, my wife Kinnari Patel, my twin brother Vishal Patel, my sister-in-law Sejal Patel, and grandmother Parvatiben Patel for believing me and having faith on me.

- Vivek Patel

Table of Contents

List of Figures

List of Tables

List of Equations

1. Abstract

Tablets are the most preferred drug delivery dosage from compares to all other delivery forms. Tablet sizes are very important to consider with respect to the patient compliance. During the early development stage, it is very important to screen out the material based on their compressibility at each plane for further formulation. There are mainly three type of crystallization method like evaporation, cooling, and antisolvent method. Slow cooling method is a useful method to determine the crystal property at a different temperature point. Metastable curves assist in identifying the nucleation point of crystal during cooling method. A limited quantity of the drug and time constraint makes it difficult to adopt trial and error techniques for optimizing tablet formulations using directly compressible excipients. Hence, characterizing the compression properties of API is desirable in the early development stage. Single macro size crystal was nucleated at a different temperature point using a slow cooling method. These crystal x, y, and z plane were identified by using the simulated PXRD pattern from the Mercury software. Crystal characterized using PXRD, DSC, and TGA. A compression stage was mounted in a x-ray diffractor for microscopic studies of crystal. Microscopic studies showed that the crystal nucleated from 65 °C saturated solution was having low Young's moduli compared to crystal nucleated at a 55 °C. Compaction simulator were used to calculate the macroscopic level studies of crystal. Force-Displacement data were used to calculate the Heckel analysis and Work-related parameters. Elastic recovery of tablet was affecting the strength of a tablet.

2. Introduction

Background

Direct compression is the easiest manufacturing option with minimum steps and least expensive technique[1]. Apart from easy process, the advantage of direct compression involves reduce capital, labor, and no use of water advantage for water sensitive API. A poorly compressible and high dose API molecule is hard to compress with direct compression. Compressibility of this type of API molecule can be improved by crystallization. The unique arrangement of molecule in three-dimensional (3-D) defines the crystal structure. The smallest 3-D arrangement of molecule is called the unit cell [2]. Crystalline material characterized by unit cell arrangement.

Crystal anisotropy is known as ability of single crystal to show different physical and chemical properties for different axes. Crystal shape and molecule packing can influence mechanical properties based on the orientation during compression. Tableting properties of API molecule can be predicted from mechanical properties of single crystal. Growing of crystal involves attachment of molecule layer to crystal face. The energy released during the attachment of this layer is called as Attachment energy[3]. Sip planes and attachment energy are inversely related. Change in d-spacing measurement helps to identify the sip planes. Visualization of crystal structure helps to identify sip planes and crystal structure. Largest d-spacing values are of sip planes.

To grow crystal with desired properties, an understanding of nucleation point of crystal in necessary. Solubility and metastable curve will give idea of nucleation point of API molecule at different temperature point[4]. The metastable zone is defined a zone between solubility curve and metastable curve providing information about controlled crystallization process. A metastable curve is the detection point of temperature at which crystal gets nucleate and detected at constant cooling rate. Nucleation of crystal take place after crossing the unsaturated region and to enter in supersaturation region with decreasing in temperature[5]. As soon as supersaturation is achieved, small cluster of molecules begin to form with increase in collision frequency of molecule[6]. The formed cluster dissolves into solution until it reaches a definite size and get stabilize. Metastable curve was identified with the help of constant cooling rate under control environment. The metastable zone width is the change in concentration between solubility curve and metastable curve limit. The metastable zone width can be calculated using equation 1:

$$lnX^{MSL} = lnX^{sol} + MSZW \quad (1)$$

Equation 1: Metastable zone width

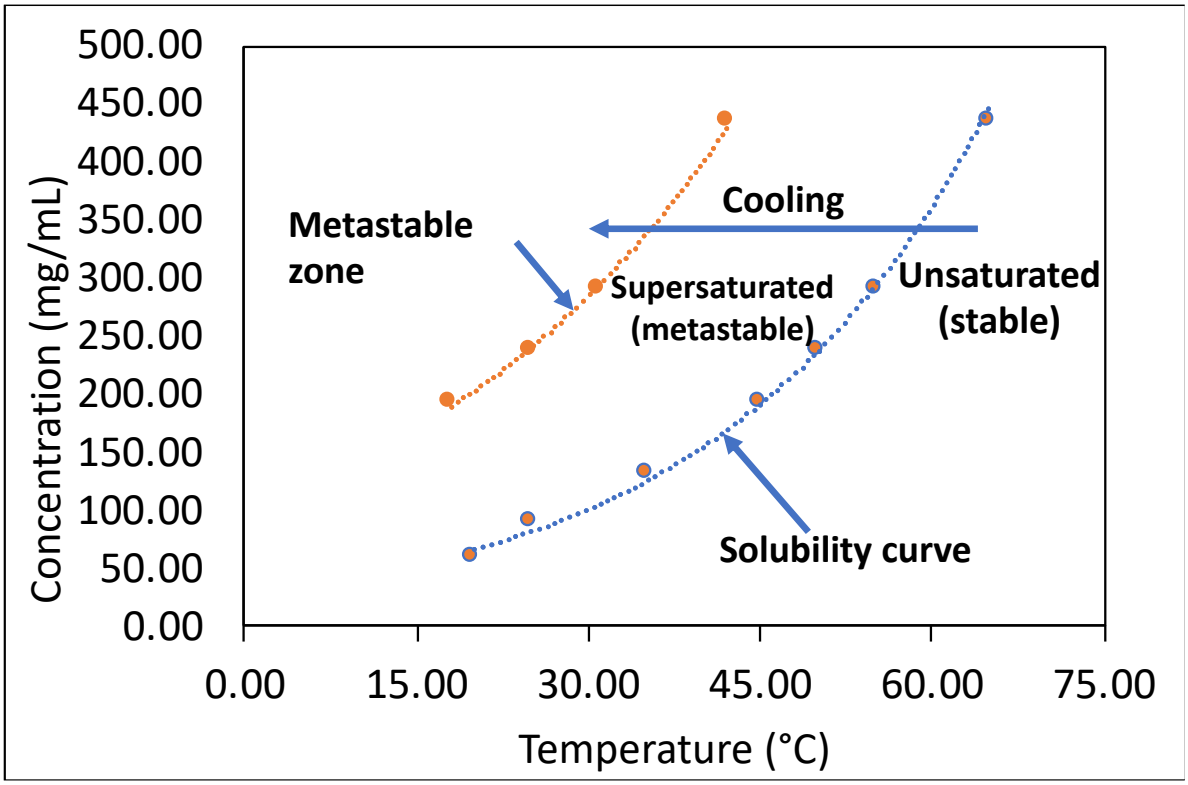

Figure 1: Solubility and metastable curve predicting metastable zone width.

Crystallization occurs when the solubility of solute reduces in solvent system. Method to reduce solubility includes: (A) Cooling (B) Antisolvent addition (C) Solvent evaporation (D) Precipitation method. Metastable curve limit was obtained using cooling method. Mettler Toledo Easy Max Crystallizer were used to obtain control condition of temperature. Saturated clear API solution were obtained with increase in temperature. Nucleation of API molecule take place with slow cooling rate and agglomeration of embryo. Large crystal forms with desupersaturation with decreasing in temperature.

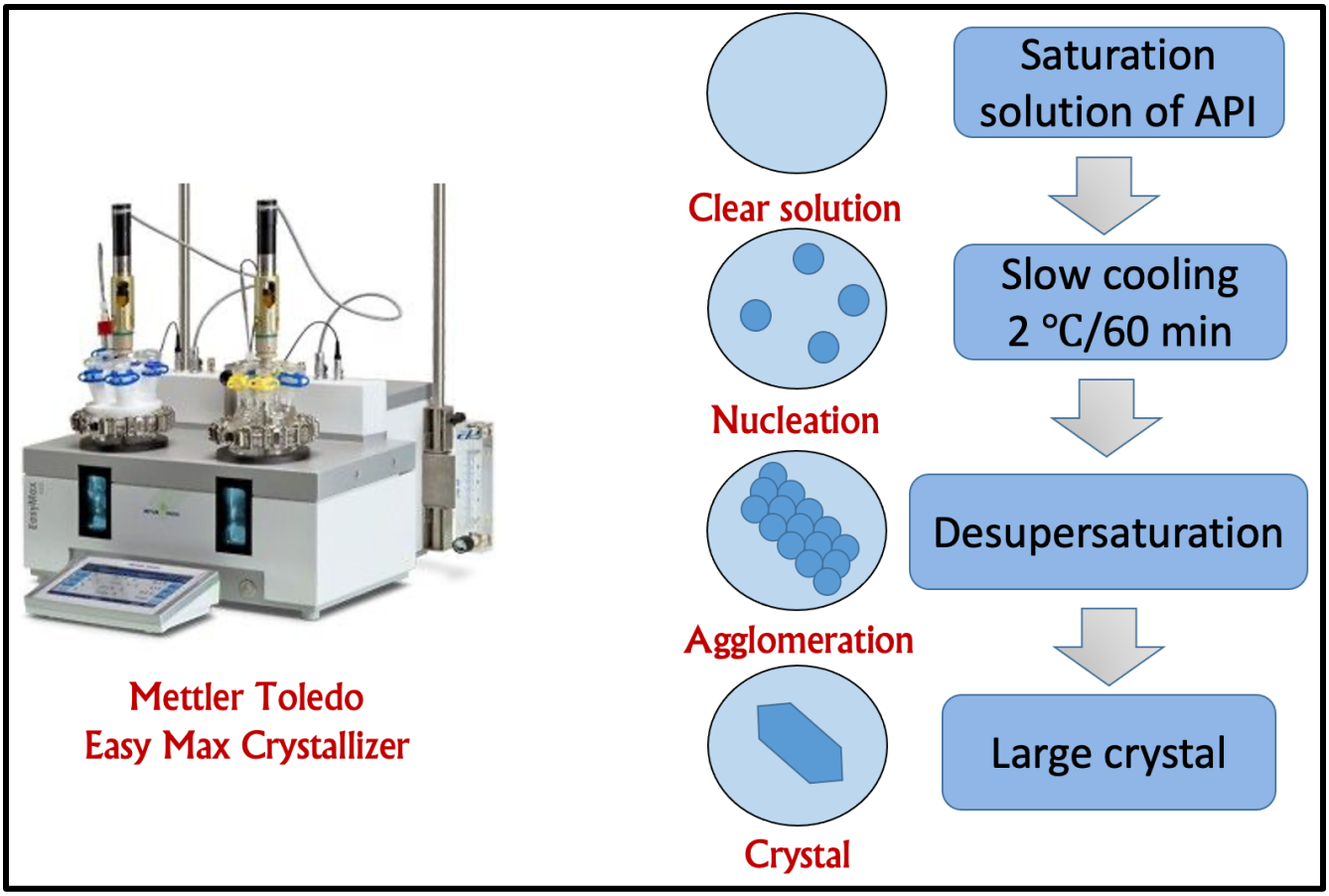

Figure 2: Single Crystal synthesis

In situ compression stage Deben Microtest mounted in powder X-ray diffractometer were used to measure crystal anisotropy of API molecule. The change in d-spacing were calculated using the diffraction pattern with stress induced on single crystal. The d-spacing value of crystal decreases with the increase of compression force. It works on principal of mechanical compression of single crystal with different compression force. To develop a relation between strain and changes in d-spacing in crystal under stress. Anisotropic Young's moduli and Bulk moduli were calculated for understanding of compressibility of API molecule. Planes were identified by calculating simulated PXRD pattern in the Mercury v3.8 software. Compressibility properties of x, y, and z plane of API single crystal was calculated and identified best compressing plane of API.

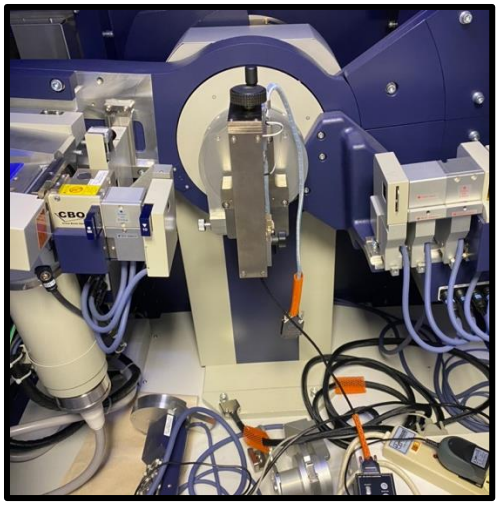

Figure 3: Compression stage mounted on PXRD

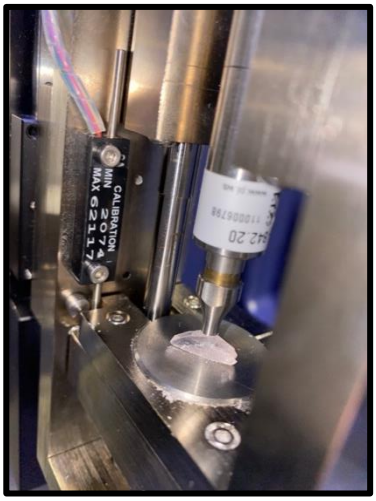

Figure 4: In situ compression stage with crystal

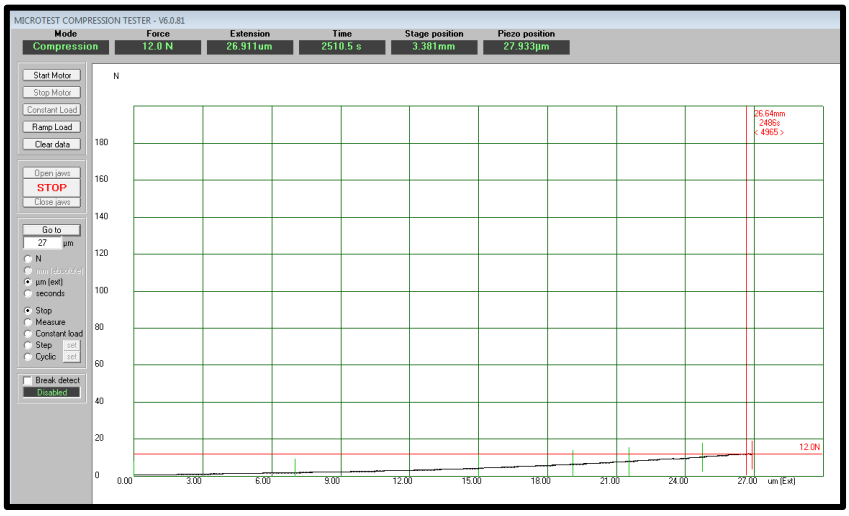

Figure 5: Microtest Compression test screen

A high dose Metformin HCl, a class of drugs called biguanides were selected for present study[7]. A type 2 diabetes mellitus drug having a dose of 500, 750, and 1000 mg. Metformin HCl d-spacing, and attachment energy will be calculated using CCDC structure data base (REFCODE: JAMRIY01). The stable form A of Metformin HCl crystal will be used for compression profile study. A macroscopic profile study of different anisotropic crystal of Metformin HCl will be performed using Compaction simulator. Macroscopic properties like compressibility, compatibility, tableting, heckel analysis, and work descriptors will be calculated by compressing crushed crystals.

3. Statement of Problem

The rapidly increasing cases of type 2 diabetes is one of the important concerns for the health care professionals. Metformin HCl approved by the U. S. Food and Drug Administration (FDA) IN 1995, since then it is mostly prescribed drug for type 2 diabetes. Metformin HCl is a poorly compressible drug, which require about 40 – 50% excipients. High daily dose (1000 to 2550 mg) of MET makes bigger size of tablet. Patients of all age complains about the size of tablet and face problems swallowing the tablet. Crushing or cutting the tablet makes patient to avoid taking pills, also alters the absorption of the medication.

Poor compressibility of MET can be improved by recrystallizing anisotropic crystal of API using metastable curve. In crystallization industry, crystal shape and size as well as habit and internal structure are important characteristics for use of the crystals. Crystallization techniques are so spontaneous it is where hard to predict the properties of crystal. Optimum crystallization process can be accomplished if the metastable zone width is known. It is important to measure supersaturating and metastability for better prediction of desired properties of crystal.

If screening of pharmaceutical materials is performed during the early stages of development that would save process time and costing of medicines. Compressibility of materials came to know at a formulation stage during the compression of materials to develop a tablet. Crystallization techniques are spontaneous, it is very hard to predict the experimental conditions when crystals are nucleated. Evaporation method of crystallization is unpredictable when the crystals will nucleate and the properties of crystal. Slow cooling method of crystallization can help to determine the temperature

at which first nucleation of crystal is observed. Metastable curve with the slow cooling method for crystallization can help in determining the desired properties of the crystals.

For development of metastable curve, solubility of API at different temperatures values are require[8]. Solubility determination at higher temperatures point is very hard to control temperature conditions during the sample handling and analysis. Special requirements of instrument are required to perform the solubility studies at different temperatures point. Easy max crystallizer can be used to determine the solubility at a controlled temperature condition. Mathematical calculations have been done to determine the solubility at a very high temperature point where we cannot be able to measure the solubility of API. Determination of mole fraction of solute in solvent at a temperature point range helps to determine the solubility at a further higher temperature point[9].

A crystalline material exhibits different properties in their physical properties in different planes. This property is known as crystal anisotropy[10]. Different molecule orientations in different planes and intermolecular interactions shows different properties of planes[11]. It is very important to analyze the anisotropic nature to understand the tableting performance of crystalline drugs. To understand the effect of compression on planes of crystal, a compression study of single crystal is required. A state of the art In-situ compression stage were developed to understand the effect of compression on a single crystal plane. Anisotropic Young's moduli calculation using the d-spacing of crystal planes can be calculated using the compression stage. Macroscopic properties of the pharmaceutical materials can be calculated using the force-displacement data. These data can be generated from the compaction simulator by compressing materials at a definite compression pressure. A macroscopic property such as yield pressure of plastic deformation, yield pressure of elastic recovery, work of compression, and work of elastic recovery. A combination of understanding microscopic and macroscopic level properties of pharmaceutical materials helps to determine the tableting performance of the material.

4. Challenges

- As a first step of developing Metastable curve, solubility value of API at different temperatures is important to measured. First challenge was to develop a method of solubility using instrument modification for better solubility determination of API. Vant's Hoff equation were used to calculate solubility of API at higher temperature with the extrapolation of plot.
- Second challenge were to develop a single big crystal using cooling method in presence of solvent. Special modification of instrument was done on crystallizer to find the solution of challenge. Different screening of solvents and crystallization process were done as a preliminary study to get a single crystal.
- Third and final task was to do compression study of single crystal using compression stage along with x-ray diffraction. The challenge was to identify the different planes of single crystal and compress at different compression force.

5. Hypothesis

Anisotropic pharmaceutical crystalline material obtained from the knowledge of metastable zone can facilitate a selection of an optimal crystalline material for better tableting performance.

6. Specific Aims

Specific Aim#1: To plot solubility curve and metastable curve limit for single crystal using cooling technique

Supporting Aims:

- To develop and validate HPLC method for Metformin HCl to analysis solubility of sample at different temperature.
- To plot a solubility curve of Metformin HCl by measuring solubility of API at different temperature in solvent system.
- To find out of nucleation temperature point of different saturated solution at different temperature.

- To determine equation of metastable zone width with the help of solubility curve and metastable curve limit.
- To screen a solvent system composition for getting a single big size crystal of API molecule.
- To evaluate the process parameters of crystallizer for growing a big size single crystal.
- To understand the effect of different cooling rate on size of crystal.
- To characterize the grown crystal by PXRD, DSC, and TGA studies.

Specific Aim#2: To measure Young's moduli of different plane using single crystal of Metformin HCl using In situ Compression stage mounted in PXRD.

Supporting Aims:

- To install and set up compression stage in Powder XRD instrument.
- To optimize the parameters of compression stage for compressing crystal along with X-ray analysis of crystal.
- To compress single crystal at different force for calculation of d-spacing using PXRD pattern.
- To find out the x, y, and z plane of crystals using Mercury v3.8 software by simulated PXRD pattern.
- To calculate d-spacing at different plane of crystal grown at different temperature.

Specific Aim#3: To measure macroscopic level properties of crystal using compaction simulator

Supporting Aims:

- To compress tablet of crushed crystal using Compaction simulator.
- To measure mechanical properties like Heckel analysis, work related parameters.

7. Study Design

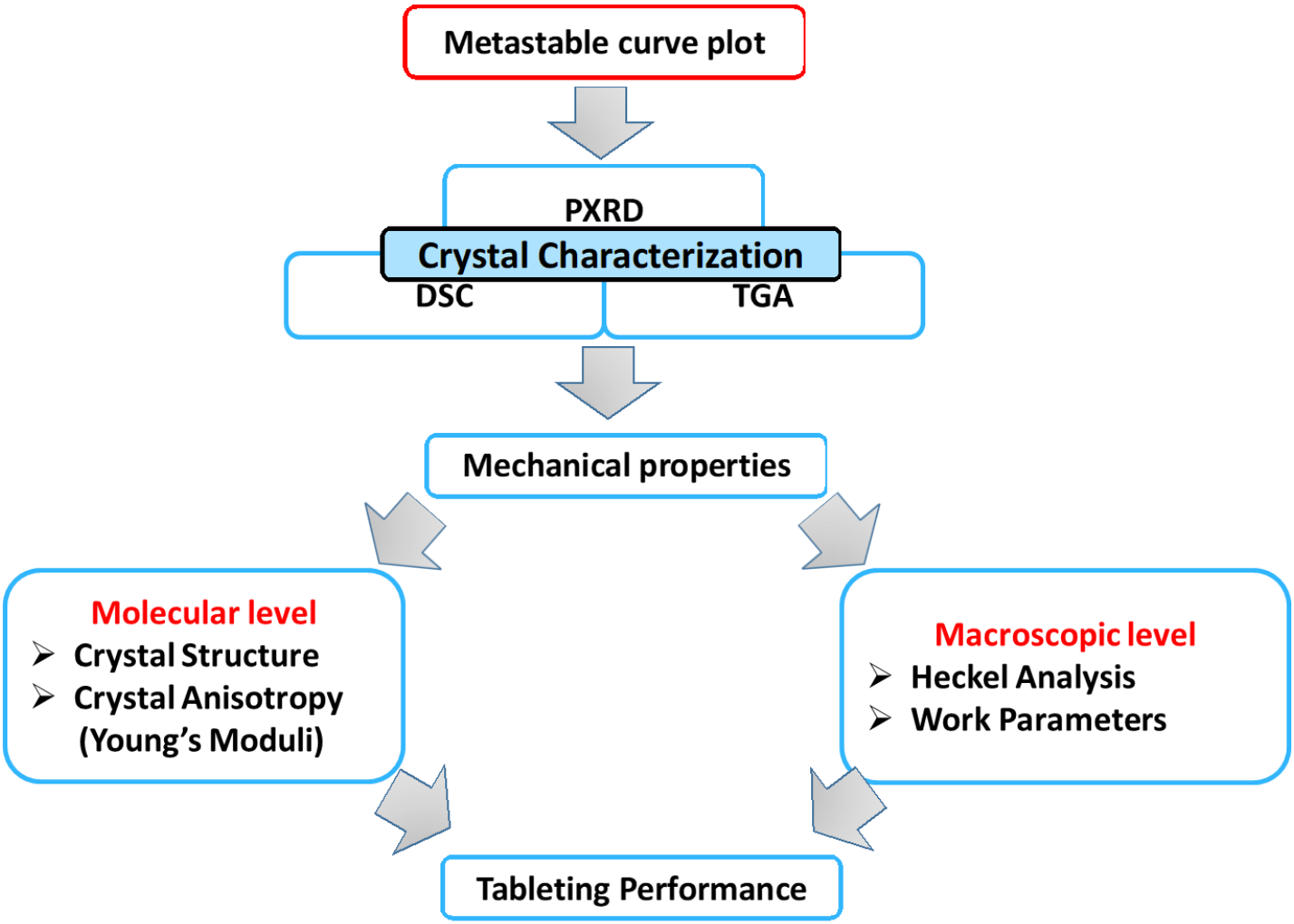

Figure 6: Experimental Design

8. Material and Methods

a. Materials

Metformin HCl (Lot No. 1910040036) was purchased from Letco ™ Medical, AL. Ethanol, Acetonitrile, and Methanol was purchased from Sigma-Aldrich, MO. Ultrapure water obtained from in-house assembly of MilliQ® IQ 7000 system (Millipore Sigma, Burlington, MA) was used for the studies.

Metformin HCl

CAS number: 1115-70-4

Chemical Name; 1,1 - Dimethylbiguanide hydrochloride

Chemical Formula: $C_4H_{12}ClN_5$

Chemical Structure:

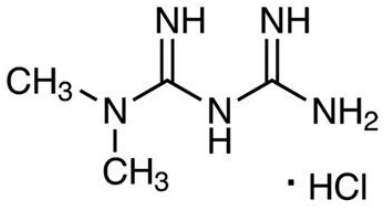

Figure 7: Metformin HCl structure

Formula weight: 165.625g/mol

Log P: 2.64

pKa (Acid): 12.4 ± 0.4

Solubility: 1.06 x 10^ mg/L at 25 °C

Metformin HCl is a biguanide class of an antihyperglycemic agent, it is first line treatment therapy for type II (non-insulin-dependent) diabetes mellitus patient [12]. Metformin HCl improves the glucose glycemic levels by decreasing hepatic glucose production, which decreases intestinal absorption of glucose and improves insulin sensitivity by peripheral glucose uptake and utilization. MET is a Class III that has high solubility and low permeability. It has oral bioavailability < 40% of the doses and it had a plasma half-life of 1.5 to 4.5 h [12]. Metformin HCl has a daily dosage of 500 - 1000 mg/day[13].

b. Methods

Solvent selection for crystallization process were done based on preliminary studies to get a single crystal. Single component and multiple components were used for solvent selection studies. Solvents like water, methanol, ethanol, acetonitrile were screened for crystallization process. Based on the results obtained and desired target results binary component of two solvents were selected for studies. Mixture of methanol: water was selected as a solvent for solubility and crystallization process. Different ratios (1:1, 2:1, and 1:2) of methanol: water was checked to get optimize ratio of solvent for studies.

Cooling rate for crystallization process were optimized by preliminary studies of running slow cooling at a different rate. Cooling rate of 2 ºC/ 60 min were selected for crystallization process for studies. Modification of process were done by taking out stirrer from the solution before starting cooling of solution to get crystals.

i. High Performance Liquid Chromatography (HPLC) Analysis

A reverse phase HPLC method was employed to quantify MET concentration in the solubility samples (Agilent 1100 series, Agilent Technologies, Cranberry, PA), which was equipped with a UV detector and an Agilent C18 (5.0 µm, 4.6 mm X 150.0 mm). The mobile phase comprised of 0.1% orthophosphoric acid and acetonitrile in the proportion of 40:60% v/v. The flow rate was 0.8 mL/min, the injection volume was 10.0 µL, and the temperature

of the column was kept at 55 °C. MET eluted at 4.6 min and was analyzed at 236 nm for all the samples. All the method suitability measurements were performed in triplicate.

System suitability are used "to verify the detection sensitivity, resolution, and reproducibility of the chromatographic system are adequate for the analysis to be done"[14]. System suitability (specificity and selectivity) was evaluated using six replicate injections of Metformin HCl (100.00 µg/mL). The recommended RSD (%) should be <2% to pass system suitability test as per the USP. Accuracy defines as "Accuracy indicates the closeness of the test results to the true values"[15]. Accuracy was determined by injecting three concentrations (20, 80, and 100 µg/mL) of Metformin HCl with three different dilutions. Each run was done in the triplicate. The recommended RSD (%) should be <2% to pass system suitability test as per the USP.

"Precision is the degree of agreement among individual test results when an analytical method is used repeatedly to multiple samplings of a homogenous sample"[15] A method repeatability was evaluated using six injections of 100.00 µg/mL with six different dilution of Metformin HCl. The recommended RSD (%) should be <2% to pass system suitability test as per the USP. "Linearity is the ability of elicit test results that are directly, or by a well-defined mathematical transformation, proportional to analyte concentration within a given range."
Range is defined as the interval between the upper and lower levels of analyte (intrusive) that have been demonstrated to be determined with a suitable level of precision, accuracy, and linearity using the method as written." The linearity of the Metformin HCl response in HPLC was tested in the range of 20 to 100 µg/mL at five different concentrations. These concentrations were 20, 40, 60, 80 and100 µg/mL. These runs were done in the triplicate. The R^2 value should be >0.999 is required to pass linearity test as per the USP.

HPLC method were validated according to the ICH guidelines requirements for linearity, system suitability, precision, accuracy, and filter binding(International Council for Harmonization (ICH), 2005).

ii. Solubility Curve

The saturation solubility of Metformin HCl at different temperature was measured using Mettler Toledo Easy Max Crystallizer. The closed assembly of instrument gives better opportunity to measure solubility at high temperature. Excess amount of Metformin HCl was added to 20.0 mL mixture of Methanol: Water (50:50) in closed jacketed beaker with paddle. The temperature of jacket was kept constant at 20, 25, 35 and 45 ºC for determination of solubility at different temperature. The paddle speed was kept constant of 200 rpm for 48 h for proper mixing of solute in a solvent. The paddle was stopped after 48 h and kept for 5 h to allow sufficient time for excess Metformin HCl powder to settle before collecting sample at a respective temperature point. The prewarmed pipette tip (20, 25, 35 and 45 ºC) was used to collect 0.1 mL supernatant from a closed jacket beaker. The collected sample were diluted with distilled water in 10.0 mL of prewarm volumetric flask [17]. The diluted sample were analyzed using validated HPLC method. All studies were performed in triplicates.

Saturation solubility of Metformin HCl at 20, 25, 35 and 45 ºC was determined using experimental studies. Van't Hoff equation was used to calculate solubility at higher temperature[18]. The solubility of API at higher temperature like 50, 55, and 65 ºC were calculated using Van't Hoff equation at extrapolate points [17]. Moles of solute and solvent were calculated based on solubility experiment were done at 20, 25, 35, and 45 ºC. Enthalpy of fusion (ΔHf) were calculated from the Differential scanning calorimetry (DSC) plot. Slope equations were used to calculate solubility of solute at a higher temperature point.

$$\ln x = -\frac{\Delta Hf}{RT}\left(\frac{Tm - T}{Tm}\right) - \ln(y) \qquad (2)$$

Equation 2: Van't Hoff equation

Where, ΔHf (J/mol) is the enthalpy of fusion. Tm (K) is the melting point of the solid solute; T (K) is the temperature of the solution; R (8.3145 J/mol. K) is the gas constant[19].

iii. Metastable Curve

Metastable zone lies between solubility curve and the metastable limit curve[20]. Metastable zone represents supersaturation condition where nucleation and crystallization event

occur[21]. Metastable zone width is the difference between solubility curve and metastable curve (nucleation curve). The region in the right of solubility curve is where API remains in a solution (Figure 1). The region to the left of metastable curve is unstable zone where uncontrolled nucleation occur. The region between solubility curve and metastable curve is the region where nucleation is not likely to occur.

A known concentration of MET was added in mixture of 40 mL of Methanol: Water (50:50) in closed jacket beaker with paddle. The temperature of jacket beaker was heated up to respective temperature (45, 50, 55, and 65 °C) as soon as possible with stirring speed of 200.0 rpm to solubilize API in a solvent. Stirring of paddle were kept running for 5 min at high temperature point. Solvent will be clear after all solutes get dissolved, and forms uniform solution. Once solution get clears, second phase of cooling initiates. The stirring of paddle was stopped, and stirrer pulled out from solution. Stirrer were holded with pipette holder from outside, to keep stirrer above the solution. Cooling rate of solution were optimized based on the initial screening studies of experiments. The temperature of jacket beaker was cooled up to 4 ºC with constant cooling rate of 2 ºC/ 60 min to crystallize single crystal from solution. As cooling approaches to lower temperature, and solution start to get in a supersaturation condition. The solution was observed for any change and temperature at which first nucleation take place was recorded. Crystal was harvested after reaching of jacket beaker temperature to 4 ºC. This study was performed at four different temperatures of 45, 50, 55, and 65 ºC to find out nucleation point. Harvested single crystal from four different temperature point were stored with care for further studies of compression.

iv. Powder X-Ray Diffraction (PXRD)

X-ray diffraction (XRD) is a technique use to determine the crystal structure of materials. XRD works by exposing a material with incident X-rays and then measuring the intensities and scattering angles of the X-rays that leave the material. Synchrotron or vacuum tube were mostly used for PXRD. The intensities of the scattered X-rays are plotted as a function of the scattering angle. XRD is use for characterization of material crystal or amorphous nature. PXRD is useful for material quantitative analysis, measuring degree of crystallinity, polymorphism, phase transition etc. XRD helps to determine the structure of crystalline

material at a molecular level. X-ray diffraction of pure MET and harvested crystal from jacket beaker at different temperature were analyzed on high-resolution X-ray diffractometer (Smartlab®, Rigaku, Tokyo, Japan). Crystals were crushed in a mortar pestle to get powder form for PXRD analysis. X-ray radiation used was generated by a copper Kα beta filter method at 40 kV and 44 mA. A 2mm deep aluminum sample holder was used, and samples were scanned from 5° to 40° 2θ with a scan step of 0.01° at the scan rate of 3° 2θ /min. PDXL software version 2 (Rigaku, Austin, TX) was used for the diffractogram analysis.

MET (Ref Code: JAMRIY01)[22] crystals structures were used from Cambridge crystallographic database, (CCDC), Cambridge UK). This simulated Pattern was used to compare the PXRD pattern of purchased MET and crystallize MET; it also was used to study and compare the structural arrangement of the molecules.

v. Thermal Analysis

1. Differential scanning calorimetry (DSC)

DSC method has been widely used in material science to measure the temperatures and heat flows associated with transitions in material as a function of temperature and time. This measurement helps to determine the physical and chemical changes that involves endothermic or exothermic process. Analysis of samples were performed by increasing or decreasing the temperature uniformly. Heat flow difference between reference and sample material are measured[23]. DSC measures the temperature difference between the sample and the reference. In standard DSC, temperature was changed linearly and in specified rate in degree per minute (°C/min). Modulated DSC works on the two simultaneous heating rates, It works on linear heating rate and with a sinusoidal heating rate[24], [25]. Physical and Chemical transition of material were characterized by DSC. Physical transition such as melting, freezing, crystallization, evaporation, vaporization, and sublimation[26]. Chemical transition includes reduction, oxidation, and degradation of material.

Simultaneous heating rates (linear and modulated) provides information on sample heat capacity. The equation that describes the heat flow signal from a DSC or modulated DSC experiments.

$$\frac{dH}{dt} = C_p \frac{dT}{dt} + f(T, t)$$

Equation 3: Heat flow equation

Where, $\frac{dH}{dt}$ = total heat flow (W/g); Cp is the heat capacity (J/cal), $\frac{dT}{dt}$ is the heating rate (°C/minute), *T is the absolute temperature, and t is the time (min).*

A close pan DSC was performed using a Q 200 DSC (TA Instruments, New Castle, Delaware, USA). Approximately 5 - 6 mg of sample (MET API and crushed crystal) was placed in an aluminum pan and weighed using microbalance. All the samples were heated from 25 °C to 300 °C, at a heating rate of 5°C per minute. Nitrogen gas was used to purge at a flow rate of 40 mL/min.

2. Thermogravimetric Analysis (TGA)

TGA was performed using Q 500 TGA (TA Instruments, New Castle, Delaware, USA). An approximately 6 -7 mg of MET API and crushed crystal were taken in a platinum pan. The pan was placed on the loading stage. All samples were heated from 25°C to 300°C, at the heating rate at 5°C per minute. Data analysis was done using Universal Analysis software version 4.5 (TA Instruments, New Castle, Delaware, USA).

vi. Anisotropic Young's Moduli from X-ray diffraction

Qualification of Compression stage was performed after carefully mounted into the PXRD. Stage height was adjusted until the X-ray diffracted on the crystal sample and crystalline PXRD pattern seen. The crystals were shaped to block shape with the help of a sandpaper. Crystal length, width and height were measured for calculating area of crystal. Figure No.8 shows a detailed view of the compression stage. Piezo electric probe is an important component of the compression stage. Block shaped crystal with known dimension were placed between probe and the stage. Once PXRD pattern shows desired plane with proper angle and height of stage, the crystal is locked with locking screw[27]. The probe is in contact with the locking screw, compression stage, top and bottom surface of crystal. The probe travels gradually certain distance in μm giving stress to exert a compression force on crystal. The probe was kept on hold in contact with crystal if desired force achieved. Diffraction

patterns are measured in planes normal to the axis of compression. Step by step with increase of compression force, diffraction pattern was collected with different force compressed on crystal at different planes. The main advantage of this technique is that X-ray diffraction pattern and probe moment to compress crystal is possible at the same time.

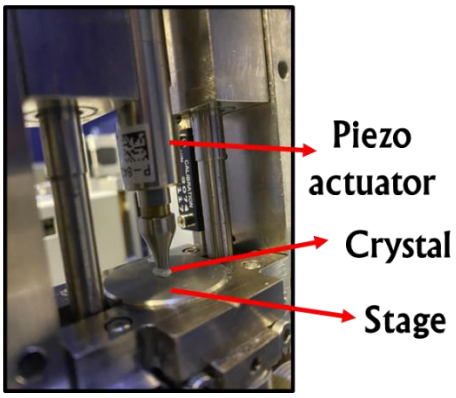

Figure 8: Crystal with stage

The degree of deformation of each plane shows its mechanical behavior. The change in d-spacing after compressing crystal will be used for calculating Young's Moduli[10]. Bragg's Law (Eq. 2) equation will be used for calculation of d-spacing [28]from the angle of diffraction [29].

$$n\lambda = 2\mathrm{d}\sin(\emptyset) \qquad (3)$$

Equation 4: Bragg's Law Equation

Where n = integer (1, 2, 3, ….., n); d = space between layer of atoms (Å); λ = wavelength of ray in (nm) nanometers; $\emptyset$ = angle of diffraction (degree)

Stress is the force applied per unit area of cross section, and strain is the ratio of change in length over initial length. A change in the d-spacing value along the given plate can be used as strain value for calculating anisotropic Young's Moduli. If the initial value of d-spacing was d_o (Å), applied force F in Newton (N), area of the cross-section of crystal A (measured using a Vernier caliper) in mm^2. A change in d-spacing and elastic Young's moduli are

inversely related. Therefore, greater the change in d-spacing, greater the probability of compressing.

$$Stress = \frac{F}{A} \quad (4)$$

Equation 5: Stress Equation

$$Strain = \frac{\Delta L}{L} = \frac{\Delta d}{do} \quad (5)$$

Equation 6: Strain Equation

$$Es = \frac{Stress}{Strain} = \frac{\frac{F}{A}}{\frac{\Delta d}{do}} \quad (6)$$

Equation 7: Young's Moduli

Elastic Young's moduli and change in d-spacing are inversely related to each other. Crystals obtained from temperature point of 65 and 55 °C were used for compression on stage. Crystals were shaped in a block shape with a sandpaper. Stage height were adjusted until the desired plane of crystal is recognized. X, Y, and Z plane of each crystal were determined, and crystals were given a compression pressure. Advantage of this technique is we can determine individual planes of crystal using PXRD.

vii. Particle Density

Density is the ratio of mass over volume. Most solids contain both inter and intraparticle spaces. Fluid displacement can calculate the volume of such materials based on Archimedes principle. Helium gas is the desired fluid for displacement as they can easily enter open voids in the particle. Helium gas also shows ideal gas behavior[30]. Gas Pycnometer consists of two cells, sample cell, and the reference cell. After helium is purged into pycnometer, the resulting pressure along with ideal gas law is used to determine particle density.

Powder particle density were measured for calculation of macroscopic properties of samples. The Particle density of MET and crystals was measured using helium displacement pycnometer (AccuPyc II 1340, Micromeritics). Helium gas was used and purged in sample

cell to analyze the density of sample. Particle densities were measured in triplicate. Samples were purged with ten repetitive cycles before final recording of data point.

viii. Powder compression

Gamlen D1000 benchtop compaction Simulator (Gamlen tableting Ltd, Nottingham, UK) was used for compression of crystal samples at Natoli Scientific, Telford, PA. Cylindrical flat-faced 6.0 mm punch were used to compact a tablet. Crystal obtained from 55 and 65 °C were crushed to get in powder form. Tablet weights were kept constant at 100 mg. Crystal powder were sieved from sieve no 30 to avoid the effect of different particle size distribution on the material compressibility. Powder was compressed using a "saw-tooth" profile at a constant pressure of 100 MPa and a compression speed of 50 mm/min. Tablets physical properties were studied at the end of the study. A total of three tablets were made at each compression pressure.

Figure 9: Gamlen compaction simulator

ix. Powder compression analysis

1. *"In-die"* Heckel analysis

Heckel plot demonstrate a linear relationship between compaction pressure and the natural logarithm of the reciprocal of the porosity of the powder bed. Heckel parameters were calculated from the force-displacement data corrected for punch-to-punch displacement[31]. The first part of the Heckel plot with low compression range indicated

rearrangement of the powder. Yield pressure of plastic deformation (YPpl) and yield pressure of elastic recovery (YPel) was measure using Heckel equation (7):

$$ln\ \frac{1}{\varepsilon} = kP + A \qquad (7)$$

Equation 8: Heckel Equation

where ε is the porosity of the compact at pressure P, k is the linear portion of compression and decompression force ranging from 20 – 80 MPa, and A is the constant. Reciprocal of the slope (k) of compression and decompression phase with a linearity of R^2 value > 0.99 gives YPpl and YPel of materials.

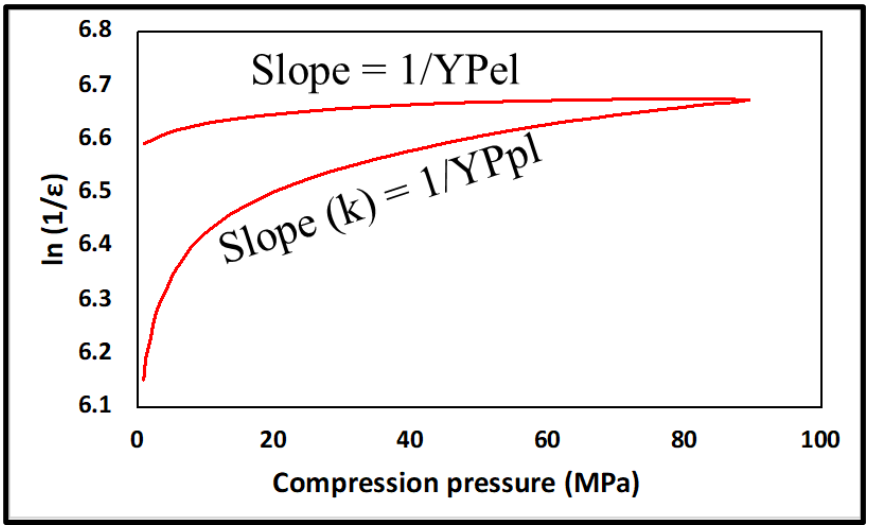

Figure 10: In-die Heckel plot graph

Figure 10 shows the graphical plot to understand the calculation of Heckel parameters. Inverse of slope of green line in plot indicates YPpl value. Inverse of slope blue line in plot shows YPel value. Material with low YPpl value indicated high plastic deformation having predominant plastic deformation properties. Powder with low YPel determines high elastic recovery having predominant elastic properties[32].

2. *Work of Compression (WOC) and Work of Elastic recovery (WOE)*

The quantification of work required to compress tablet during the compression and decompression phase of materials. Work of compression (WoC) and Elastic recovery (WoE) value were calculated using force-displacement data recorded during the compression

cycle. Area under curve (AUC) of WoC and WoE was calculated using trapezoidal rule on force (kN) vs powder displacement (mm) graph.

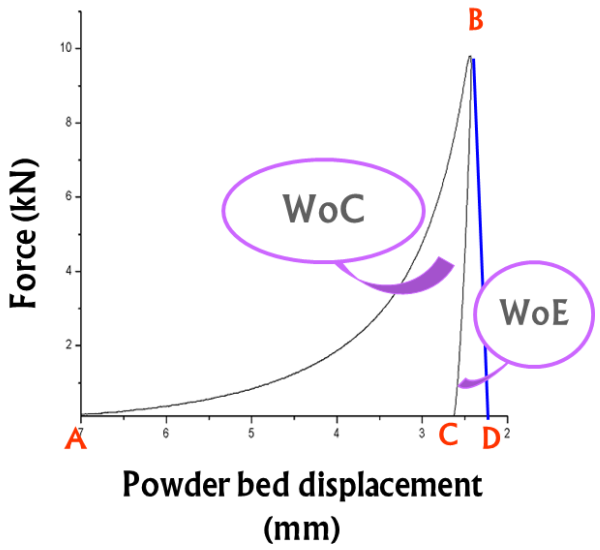

Figure 11: Work-related parameters

Figure 11 is a schematic representation of upper punch force displacement profile. The area covered by ABD is called the work of displacement. The area under CBD is called the WoE. The difference between the areas of ABD and CBD is WoC. Materials behaves mainly three different types of deformation namely plastic and elastic. Plastic material remains in deformed condition after compression. Perfect elastic material completely recovers to original position in post compression. Pharmaceutical materials are not perfectly plastic or elastic. Material behaves as a predominantly plastic, elastic, or fragmenting material (Figure 12). These calculations were done on basis of punch displacement data obtained form In-die compression. This recovery or deformation of material after compression is called as apparent work of elastic recovery or apparent work of plastic deformation[33].

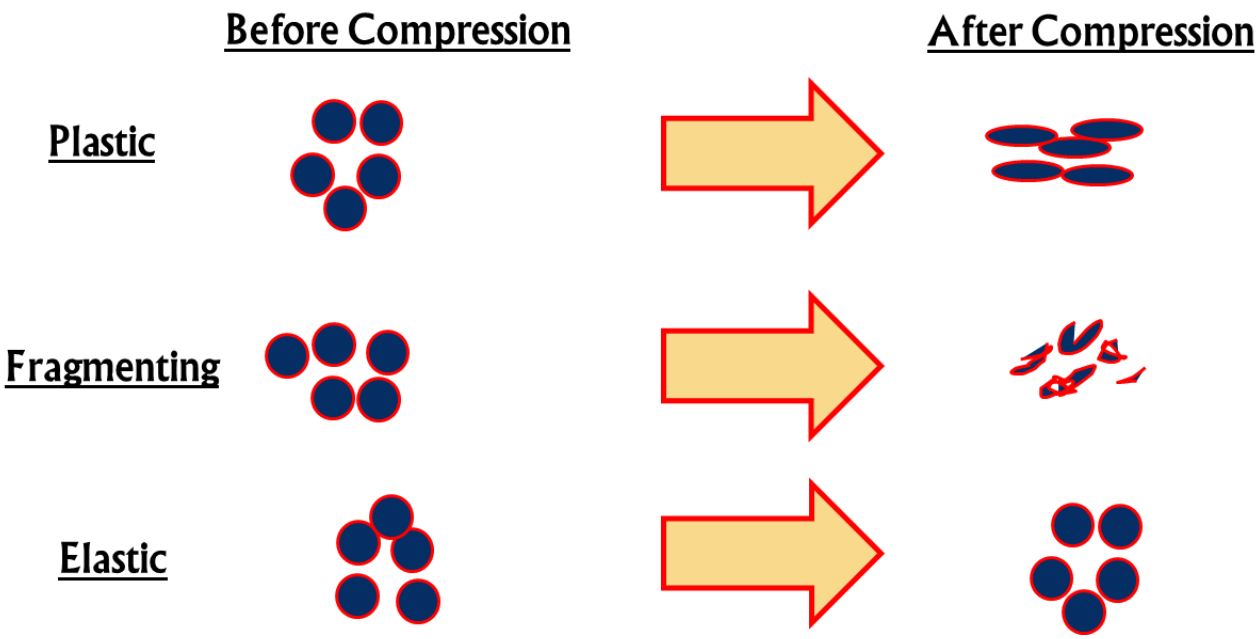

Figure 12: Material behavior during compression

x. Tablet mechanical strength (TMS)

Breaking force of tablets were measured using a Natoli hardness tester. Tablet dimension like diameter ang height were measures using Mitutoyo micrometer. Tablet mechanical strength[34] were calculated using the Equation 8:

$$TMS = \frac{2F}{\pi DT} \quad (8)$$

Equation 9: Tablet mechanical strength

Where F is the tablet breaking force (N), D is the tablet diameter (mm), T is the tablet thickness (mm).

xi. Statistical analysis

One-way Analysis of Variance (ANOVA) was performed with α value was set to 0.05 for analysis. ANOVA analysis was performed in Microsoft Excel using data analysis tool pack.

9. Results

i. High Performance Liquid Chromatography (HPLC) Analysis

Metformin HCl was eluted at 1.90 min. Linearity R^2 value of MET method validation was 0.9997. The six replicate injections of 100 µg/mL concentration of metformin showed the RSD (%) < 2% as per the requirement and passed the system suitability test (Table 1).

Table 1: System suitability of Metformin HCl

SYSTEM SUITABILITY	
Conc. (µg/mL)	Area
100.00	2700.00
100.00	2634.40
100.00	2635.30
100.00	2646.30
100.00	2628.60
100.00	2634.40
Average	2646.50
STD.Dev	26.84
%RSD	1.01

Accuracy study of HPLC method validation were performed at three different concentrations (20, 80, and 100 µg/mL). The different concentrations injection of metformin with different dilutions showed RSD (%) < 2% as per the requirement and passed the accuracy test (Table 2).

Table 2: Accuracy of Metformin HCl

ACCURACY					
Conc. (µg/mL)	Area	Conc. (µg/mL)	Area	Conc. (µg/mL)	Area
20.00	555.10	80.00	2067.50	100.00	2624.60
	540.10		2091.70		2729.10
	545.30		2063.20		2685.80
Mean	546.83	Mean	2074.13	Mean	2679.83
Std. Dev	7.62	Std. Dev	15.36	Std. Dev	52.50
%RSD	1.39	%RSD	0.74	%RSD	1.96

Precisions study was performed at 100 µg/mL with six injections at each different dilution sample preparations. The six injection of 100.0 µg/mL concentration of metformin showed RSD (%) < 2% and passed the precision test (Table 3).

Table 3: Precision of Metformin HCl

PRECISION	
Conc. (µg/mL)	Area
100.00	2592.70
100.00	2619.70
100.00	2617.80
100.00	2627.10
100.00	2607.90
100.00	2593.20
Mean	2609.73
Std. Dev	14.37
%RSD	0.55

Linearity and range study of method validation was performed on range of concentrations from 20 to 100 µg/mL. The concentration of 20, 40, 60, 80, and 100 µg/mL showed linearity response of the metformin with R^2 value >0.999 and meet the requirement to pass the linearity and range test (Table 4).

Table 4: Linearity of Metformin HCl

LINEARITY			
Metformin Conc. (µg/mL)	**Area_1**	**Area_2**	**Area_3**
20.00	555.10	531.80	545.30
40.00	1050.30	1077.20	1110.90
60.00	1563.70	1564.90	1623.00
80.00	2067.50	2091.70	2063.20
100.00	2624.60	2729.10	2593.80

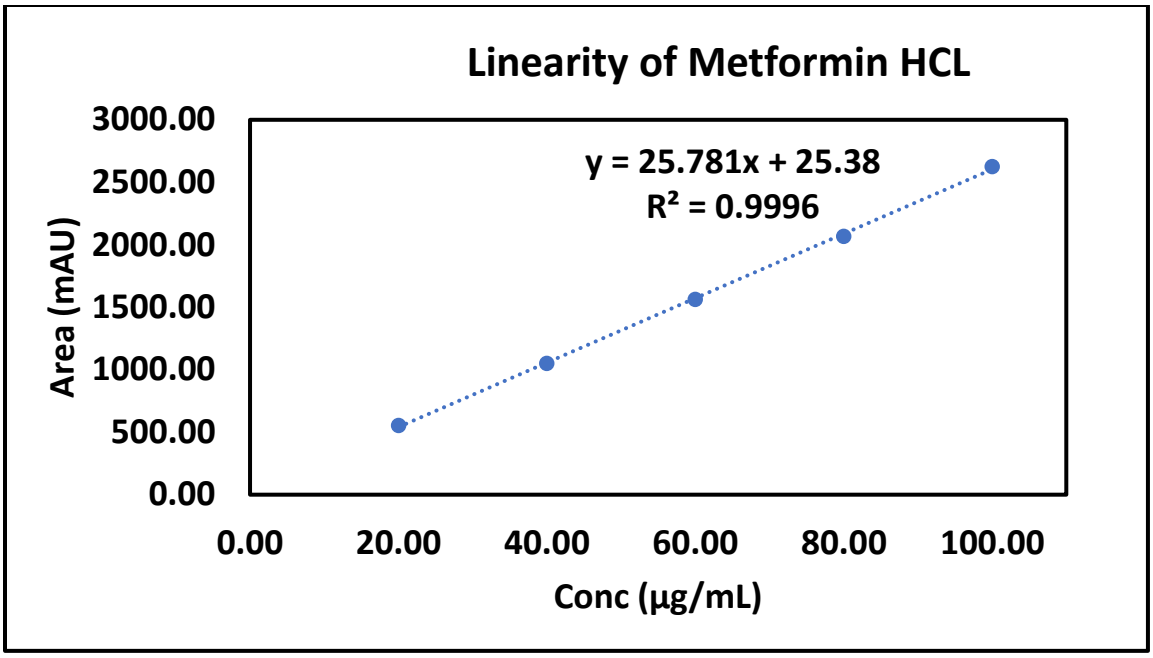

Figure 13: Linearity of Metformin HCl

% RSD value of Accuracy, precision, and system suitability were less than 2.0% as per ICH Q(2) guidelines. Solubility samples were run with the developed and validated HPLC method.

ii. Solubility Curve

To develop the model for metastable limit, the knowledge of solubility process is important[35]. Easy max crystallizer was used to measure the solubility of MET at different temperatures point (20, 25, 35, and 45 °C) to maintain close environment. Excess amount of MET was kept in different temperature points solvent for 48 h. Samples was collected at a temperature point of 20, 25, 35, and 45 °C was injected in HPLC for quantitative analysis of MET. The solubility of Metformin HCl were found to be 58.94, 80.43, 132.30, 192.52 mg/mL at 20, 25, 35, 45 °C respectively.

Table 5: Solubility data of Metformin HCl

Temp	Run No	Area	Dilution factor	Area	Concentration (µg/mL)	Concentration (mg/mL)	Average (mg/mL)	SD
20 ℃	1	19205.30	100.00	1920530.00	61303.20	61.30	58.94	3.03
	2	18794.30	100.00	1879430.00	59991.31	59.99		
	3	17396.00	100.00	1739600.00	55528.04	55.53		
25 ℃	1	1015.40	2500.00	2538500.00	81028.37	81.03	80.43	0.62
	2	999.80	2500.00	2499500.00	79783.52	79.78		
	3	1008.50	2500.00	2521250.00	80477.76	80.48		
35 ℃	1	1690.70	2500.00	4226750.00	134916.14	134.92	132.30	2.48
	2	1654.30	2500.00	4135750.00	132011.49	132.01		
	3	2036.00	2000.00	4072000.00	129976.63	129.98		
45 ℃	1	2339.30	2500.00	5848250.00	186673.30	186.67	192.52	13.13
	2	2297.30	2500.00	5743250.00	183321.77	183.32		
	3	2601.00	2500.00	6502500.00	207556.51	207.56		

Solubility of MET at 50, 55, and 65 °C was calculated using Van't Hoff Equation. Plot of log mol fraction of solute (x) vs temperature (K) was plotted to get an equation. Solubility data measured at four different temperatures point were used to plot the curve. Moles of mixture of solvents and moles of solutes were calculated based on molecular mass were used to do calculations of equation. Enthalpy of fusion ΔHf (J/mol) and Tm (K) values were -52783 and 503.77 respectively.

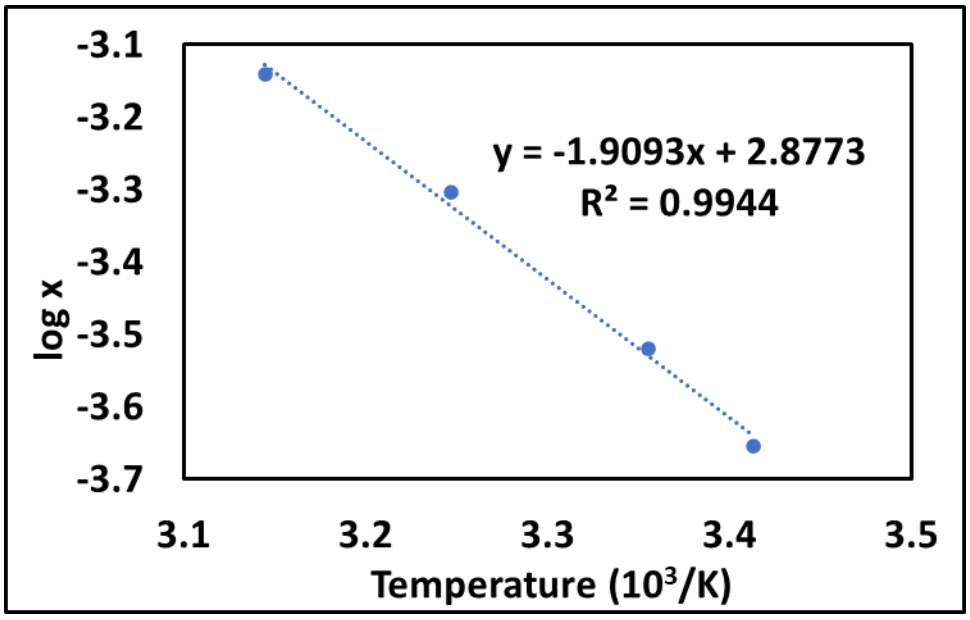

Figure 14: Van't Hoff plot of Metformin HCl

Saturation solubility measured at different point of temperature is an important component for plotting a metastable curve. Based on the measured solubility at four temperature point,

solubility at extrapolate temperature point were calculated using Van't Hoff Equation. The calculated solubility at 50, 55, 65 °C were 238.78, 291.85, and 436.77 mg/mL respectively. Solubility curve of MET was plotted (Figure 15). Exponential trendline were used to get a solubility equation at different temperatures point. Solubility equation obtained from the plot found to be:

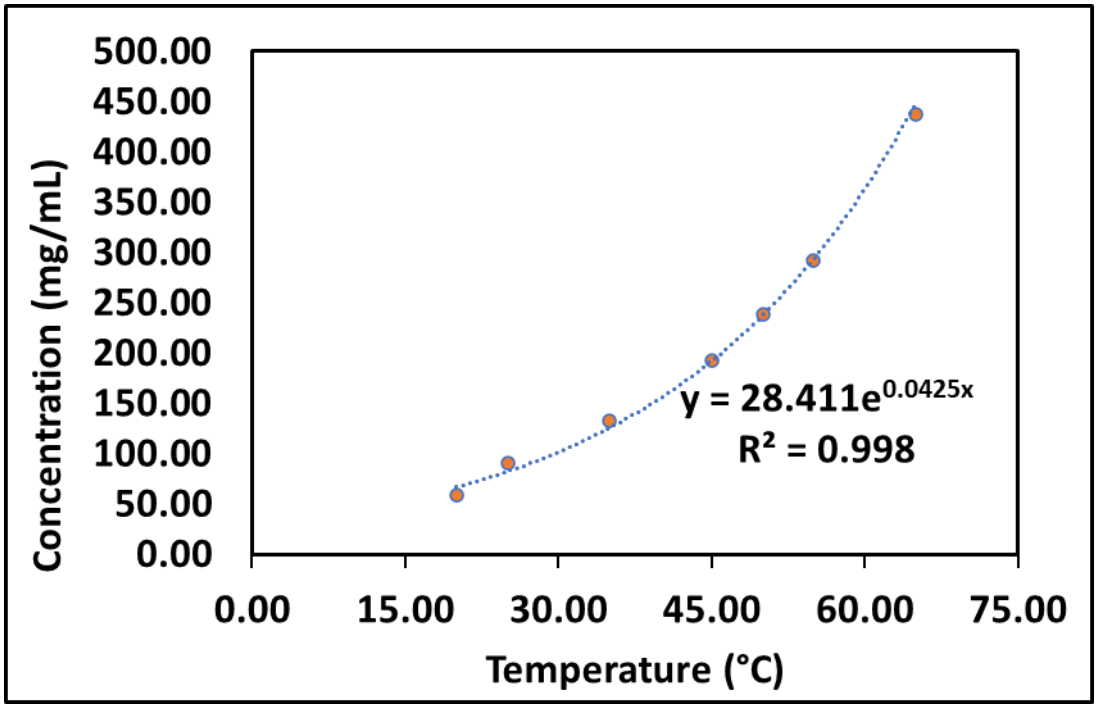

Figure 15: Solubility curve of Metformin HCl

iii. Metastable Curve

The concentration of MET at different temperatures points were obtained from the solubility curve as an important component to develop a metastable curve. Saturation solution of MET was developed at a respective temperature point depending on the solubility. Temperature point of 65, 55, 50, and 45 °C was selected to determine the nucleation point and develop a metastable curve. Saturated solutions were cooled at a slow colling rate to nucleate a crystal and grow a big single crystal. Saturation solutions were kept in a constant condition without disturbing the motion. Temperature probe were inside the saturation solution to keep the measure and control the temperature of jacket. The solution was cooled at a cooling rate of

2 °C/ 60 min from the respective four different temperature starting points to the 4 °C. The nucleation temperature point was recorded where the crystal we can observe. Saturated solution at 65, 55, 50, and 45 °C showed crystal nucleation at a temperature point of 42.25, 31, 25, and 18°C, respectively (Figure 16).

Figure 16: Nucleated crystals at different temperature points of Metformin HCl

Solubility curve and nucleation curve were plotted in concentration vs temperature plot (Figure 17). Orange color line curve represents the metastable curve. Blue color line curve shows the solubility curve. An exponential curve was fitted to both solubility and metastable curve to get equation. The range of values difference between the two curves represents the metastable zone. The distance between the solubility curve and the metastable curve represents the metastable zone width. By rearrangement of the equations in figure 17, the following equations were obtained:

$$\ln Y = 0.0425T + \ln 28.414 \quad (10)$$

Equation 10: Solubility equation of Metformin HCl

$$\ln Y = 0.0339T + \ln 103.19 \quad (11)$$

Equation 11: Metastable curve equation of Metformin HCl

Where, Y represents the mole fraction of Metformin HCl and T is the temperature for both solubility and metastable curve.

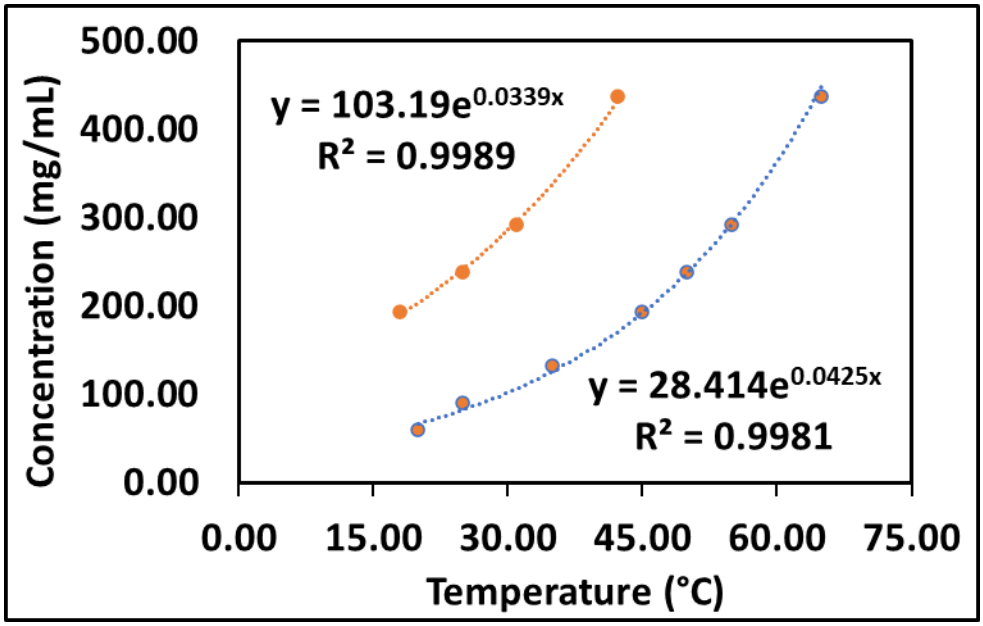

Figure 17: Metastable curve of Metformin HCl

iv. Powder X-ray Diffraction (PXRD)

Metformin HCl and crystal obtained from the metastable curve were analyzed and compared with the PXRD pattern. Experimental PXRD of MET showed the crystalline peak at 2Θ values of 12.20°, 17.62°, 22.32°, and 24.50°. This pure MET pxrd pattern shows the stable form A[36]. The PXRD pattern of crystal harvested from metastable curve at different temperature were also overlaying to pure API pattern confirming the recrystallization of Metformin HCl. Figure 18 shows the overlay of pure metformin HCl, and crystals obtained from the metastable curve. The PXRD pattern are perfectly overlaying to each other demonstrating the crystals are Metformin HCl. The simulated PXRD pattern (Figure 19) were used to determine planes of crystal from Mercury 2021.1.0 (CCDC, Cambridge, UK).

Metformin HCl (Reference code: JAMRIY01) were used to calculate PXRD pattern[37]. Unit cell of metformin HCl were shown in figure 20.

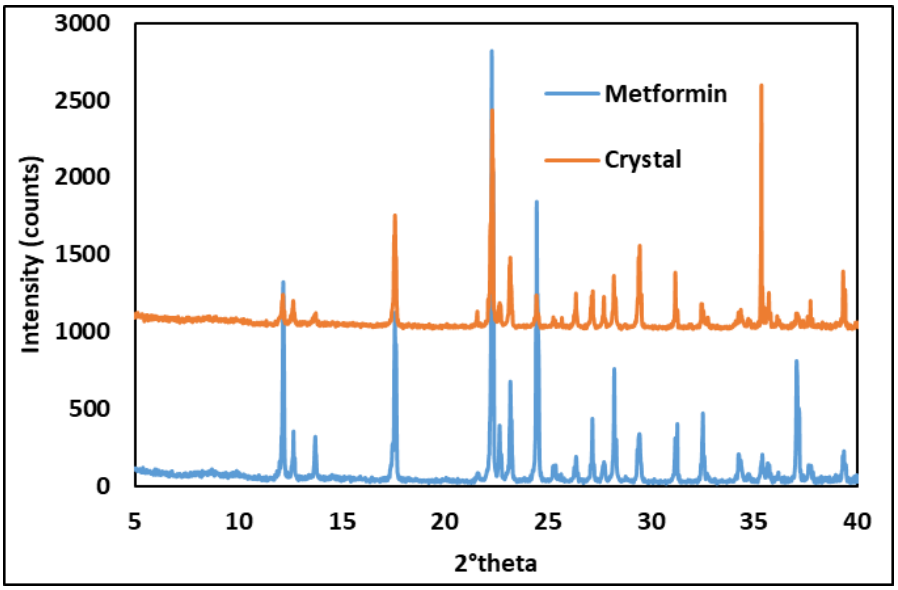

Figure 18: Experimental PXRD pattern of Metformin HCl API and Crystal

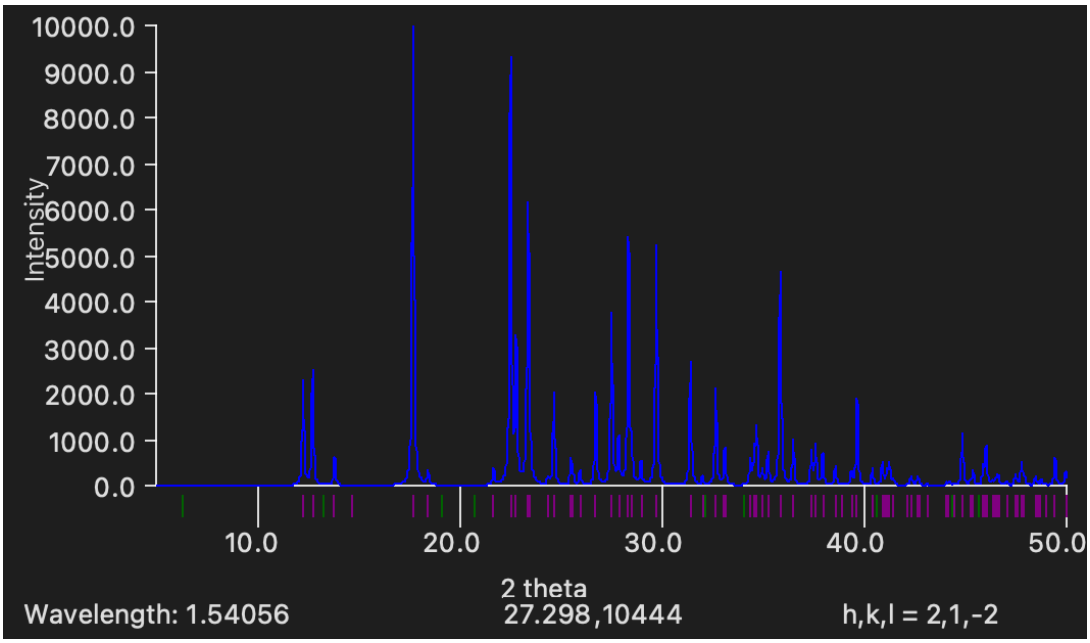

Figure 19: Simulated PXRD pattern of Metformin HCl (Ref code: JAMRIY01)

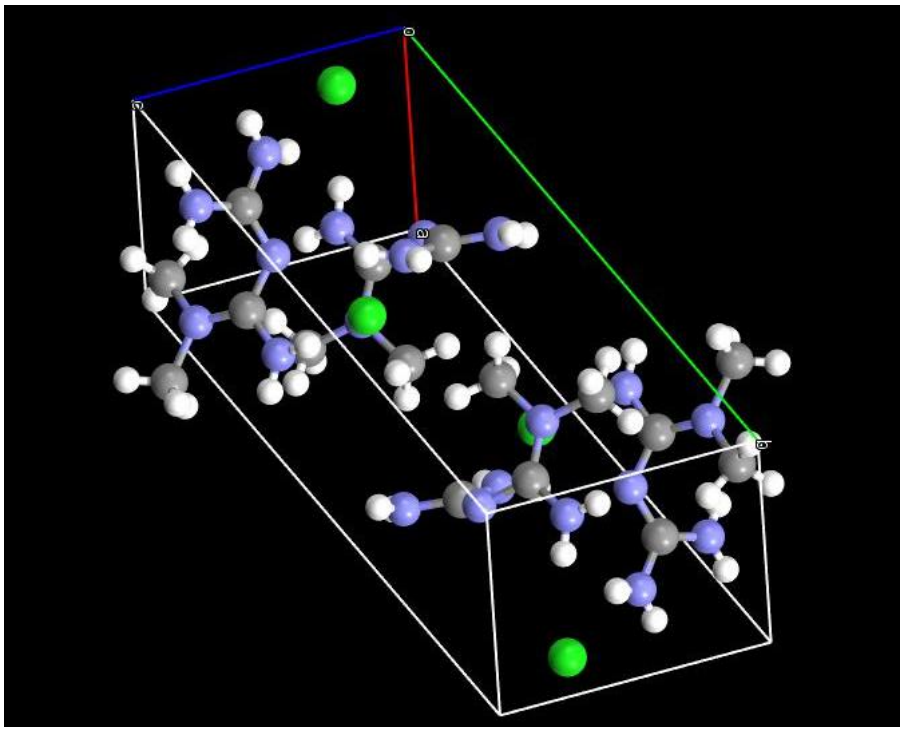

Figure 20: Unit cell of Metformin HCl

v. Thermal Analysis

1. Differential scanning calorimetry (DSC)

The DSC thermogram of Metformin HCl showed an endothermic peak at 227.80 °C (Figure 21). The peak corresponds to melting point. MET CRYSTAL obtained from metastable curve showed an endothermic peak at 227.72 °C. The overlay DSC thermogram shows similar pattern which confirms recrystallization of Metformin HCl. There was no loss of weight observed at this temperature in TGA (Figure 22) which shows that this is an endothermic peak due to the melting of a pure compound. Other endothermic peaks in DSC thermogram demonstrates the degradation of MET. There is no endothermic peak observed below 100 °C, which shows there is no hydrate in crystals obtained from the nucleation curve (Figure 21). Enthalpy of fusion for Metformin HCl and MET crystal obtained from the DSC plot are 273.2 and 295.9 J/g, respectively.

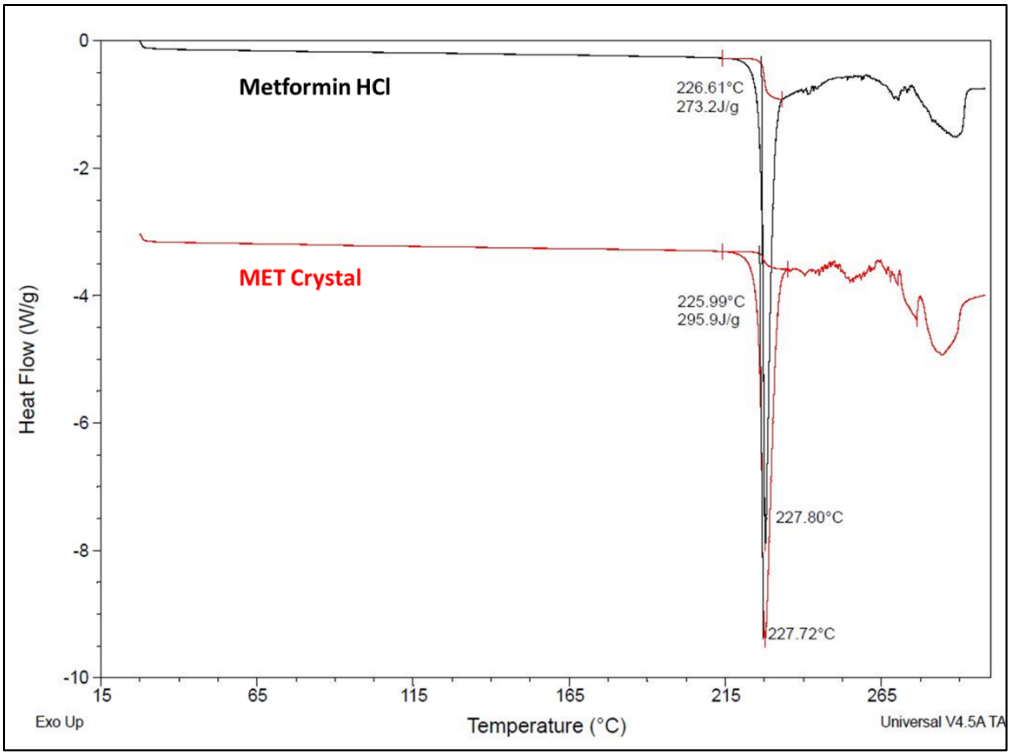

Figure 21: DSC thermogram of Metformin HCl and MET crystal

2. Thermogravimetric Analysis (TGA)

TGA overlay of Metformin HCl and Met crystal showed no solvent loss on heating. MET and crystal obtained from nucleation curve start degrading around 227 °C.

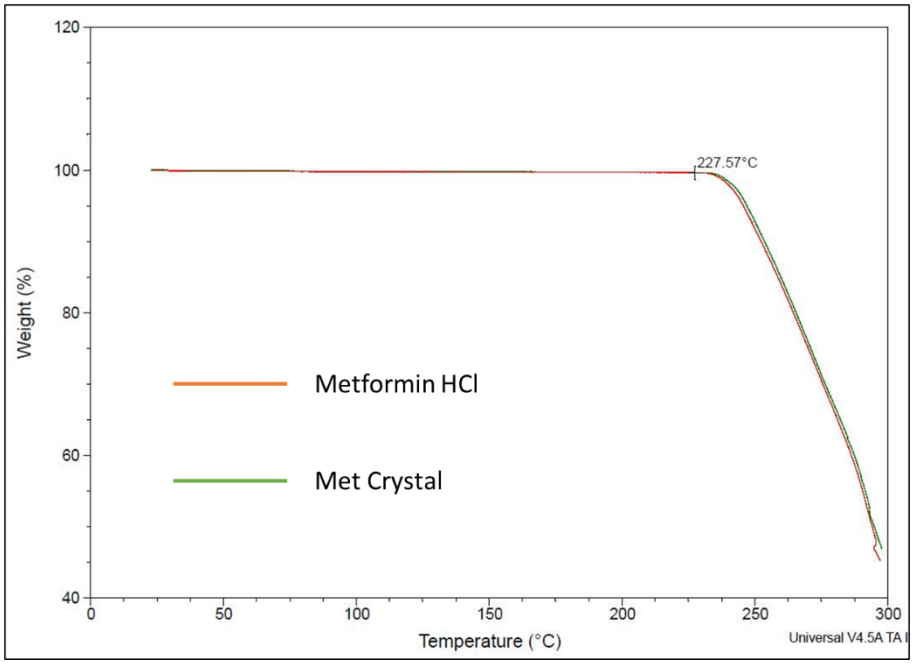

Figure 22: TGA overlay of Metformin HCl and MET crystal

vi. Anisotropic Young's Moduli from X-ray diffraction

Young's moduli were calculated from the values of d-spacing with the measurement of stress and strain. Young's moduli decrease with increasing in the compression force on the single crystal. Three representative planes x, y, and z were chosen for crystal obtained at two temperature points of 55 and 65 °C. Planes of crystals were determined from the simulated PXRD patterns obtained from the Mercury software. Planes x, y, and z of crystals at 65 °C were (1,0,0), (0,1,0), and (0,0,1) respectively (Figure 23). Similarly, crystal at 55 °C x, y, and z planes were (2,4,-2), (0,0,2), and (0,0,2) respectively (Figure 24). All crystals were shaped in a block shape with a known dimension's values. For each plane of crystal different crystals were selected for a compression study test using X-ray diffraction.

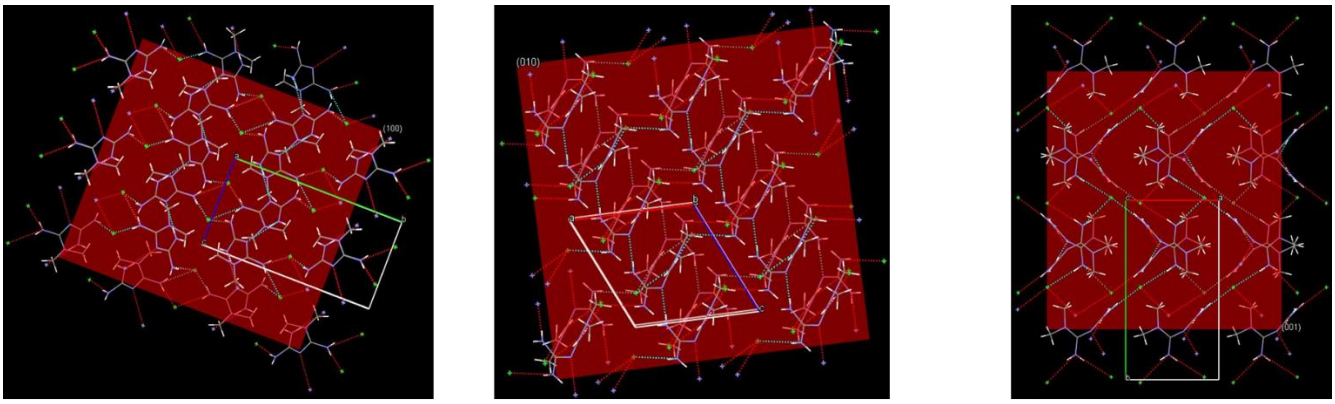

Figure 23: Planes of crystal at 65°C

Diffraction studies were performed of each crystal at 0 N force, before started applying compression force to planes of crystals. X- plane of 65 °C crystal was compressed from 0 N compression force to 8 N. Similarly, y and z plane of 65 °C crystal was compressed from 0 to 4 N compression force. The x-plane of 65 °C crystal showed lowest Young's moduli compare to other two planes of crystal (Figure 23). The z-plane showed highest Young's moduli compared to two different planes. The Young's moduli of x, y, and z planes were found to be 66.64, 152.75, and 144.28 MPa, respectively for 65 °C crystals. These data suggests that x-plane of 65 °C crystals are more compressible compared to other two planes. There is larger d-spacing in x-plane compared to other planes forming a softer plane.

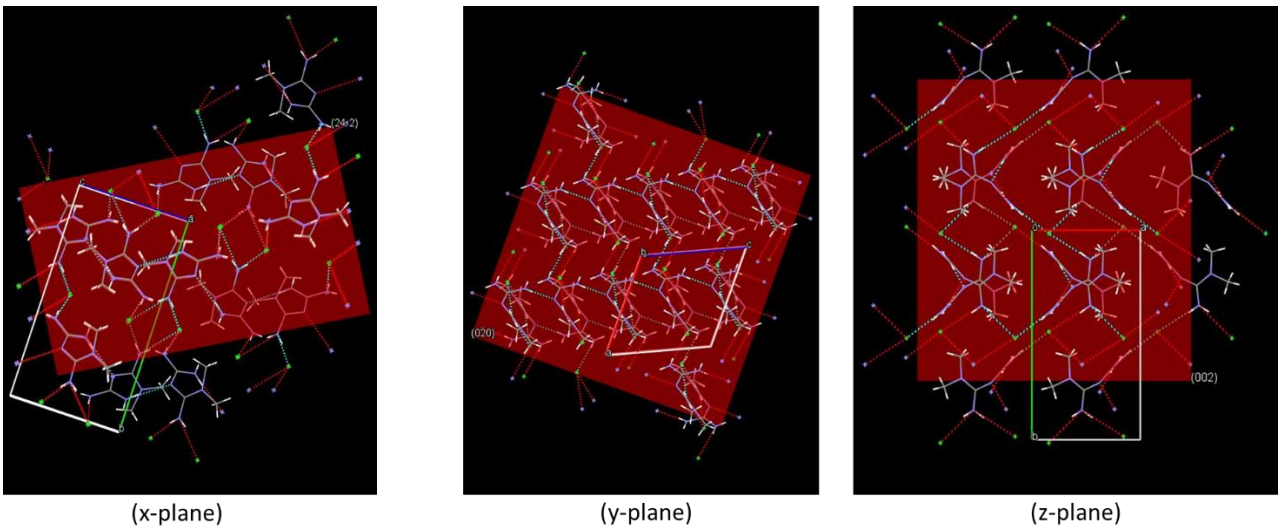

Figure 24: Planes of crystal at 55 °C

Similar trends were observed for crystals at 55 °C. The x-plane showed lowest Young's moduli compared to other two planes. The z-plane showed highest Young's moduli compared to all other planes. Young's moduli of crystal planes at 55 °C are significantly more compared to planes of crystal at 65 °C (Figure 23). The z- plane of crystal at 55 °C had greater Young's moduli compared to z- plane of crystal at 55 °C. The z-planes of both crystal points have a greater resistance to compression. X-plane of crystals have a higher probability of exhibiting slip planes[10].

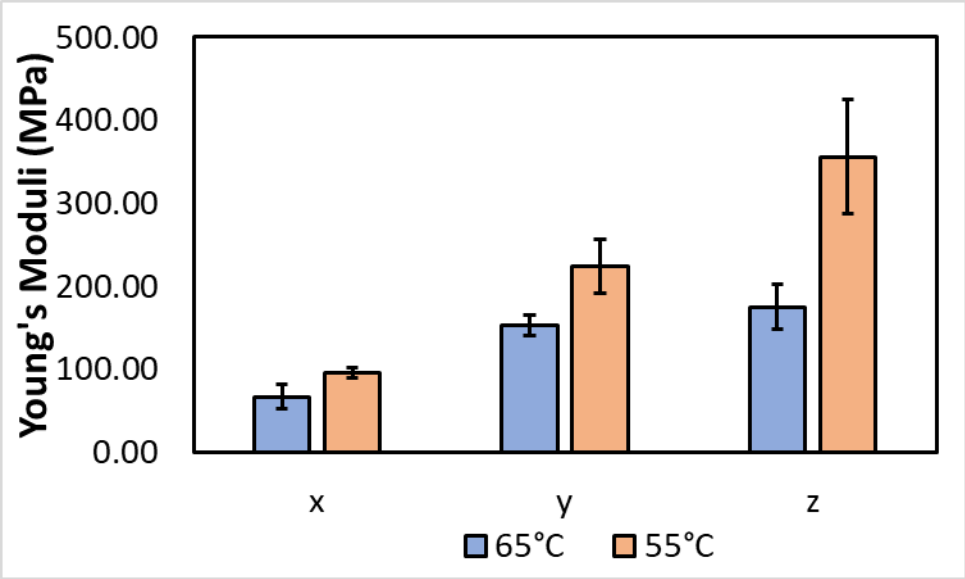

Figure 25: Young's moduli of 65 and 55 °C crystal planes

vii. Particle Density

Crystal powder were sieved from the sieve no #30 before measurement of particle density to avoid particle size difference on the helium pycnometer. Particle density of crystal nucleated at 65 and 55 °C was 1.362 ± 0.002 and 1.361 ± 0.002 g/cc, respectively.

viii. Powder compression analysis

1. *"In-die"* Heckel analysis

Heckel analysis was performed during compressing a sample at 100 MPa to understand the deformation tendencies of materials. Heckel plot of crystal at 55 and 65 °C were shown in figure 26. The plot pattern demonstrates that Metformin HCl have a greater tendency of elastic recovery[31], [32]. The YPpl and YPel value of crystal at 65 °C was calculated as

58.382 ± 1.193 and 109.715 ± 6.047, respectively. These values were found to be lower compared to crystals at 55 °C (Figure 27). The YPpl and YPel value of crystal at 55 °C was calculated as 67.468 ± 1.901 and 137.694 ± 2.864, respectively. Crystal at 55 °C have a greater tendency of compression compared to 65 °C nucleated crystals. There were statistical significance differences were observed between values, with a P-value less than 0.05.

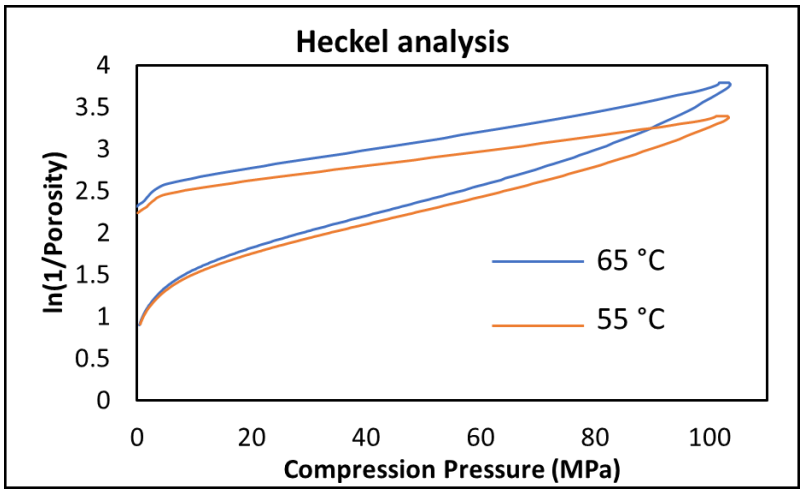

Figure 26: Heckel plot of crystals at 55 and 65 °C

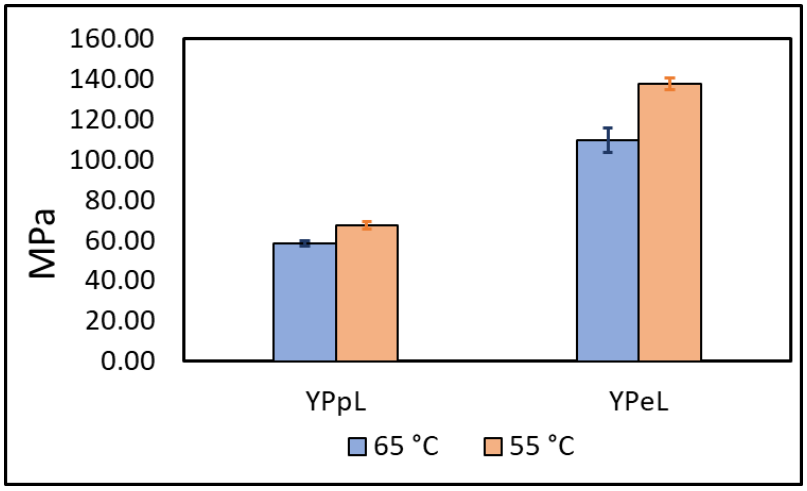

Figure 27: YPpl and YPel vales of crystals

2. Work of Compression (WOC) and Work of Elastic recovery (WOE)

WoC and WoE results of both temperature point crystals are represented in Figure no 27. The work of compression for crystal at 55 °C was found to be more compared to crystal at 55 °C. The work of elastic recovery found to be oppositely difference. The

WoC and WoE of crystals at 65 °C are 0.614 ± 0.12 and 0.200 ± 0.003, respectively. WoE of crystals at 65 °C was more compared to crystals at 55 °C. The WoC and WoE of crystals at 55 °C was 0.622 ± 0.007 and 0.198 ± 0.005, respectively. There were no statistical significance differences between the WoC and WoE values.

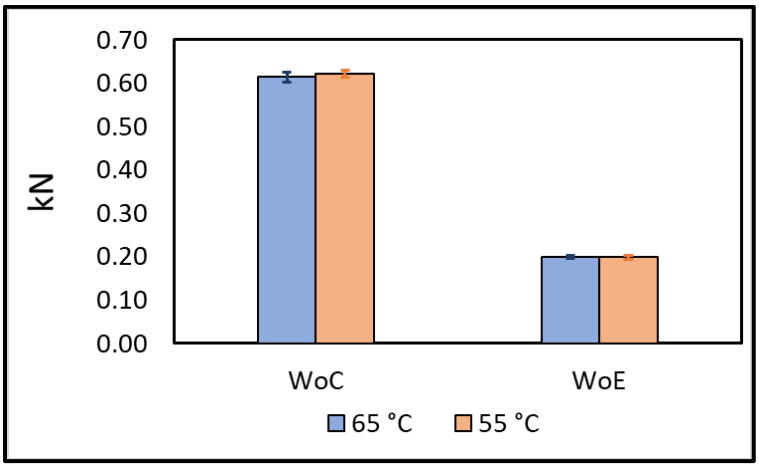

Figure 28: Crystals apparent WoC and WoE

ix. Tablet mechanical strength (TMS)

Tablets compressed at 100 MPa for crystal at 55 and 65 °C were used to understand the effect of material on strength of tablet. TMS of crystal at 65 °C was less compared to crystals at 55 °C. TMS values demonstrates that YPel is predominantly affecting the strength of tablets compared to YPpl. As YPel value of crystal at 65 °C were found to be significantly lower than crystals at 55 °C. There was statistical significance difference between the TMS values, with a p-value less than 0.05.

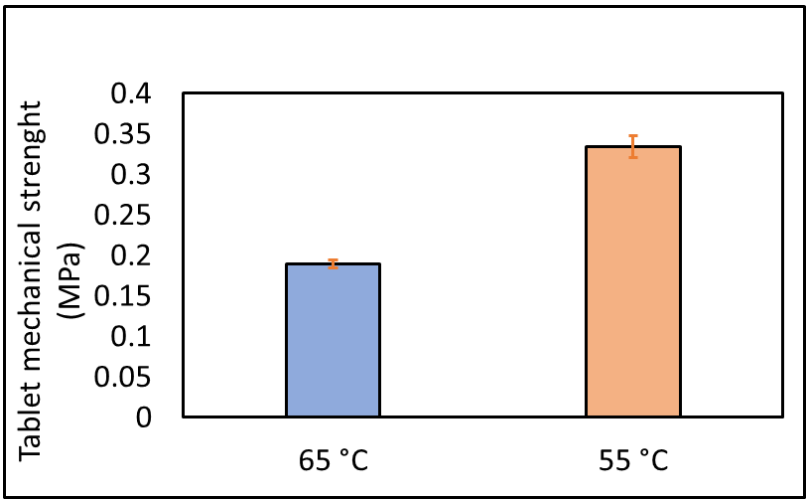

Figure 29: Tablet mechanical strength of crystals at 65 and 55 °C

10. Conclusion

Solubility curve equation were developed by measuring the solubility of MET in methanol: water (50:50 %w/w) at different temperature points of 20, 25, 35, and 45 °C. Van't Hoff equation was used to calculate the solubility at higher temperatures points of 50, 55, and 65 °C. Accuracy, precision, system suitability, and linearity of HPLC method development were found to be less than 2 %. Crystallization method of slow cooling was developed to grow a macro size crystal at different temperatures points. Cooling rate of 2 °C/60 min was used to grow a single macro size crystal in methanol: water (50:50 %w/w) solvent. Saturated solution at 65, 55, 50, and 45 °C showed crystal nucleation at a temperature point of 42.25, 31.00, 25.00, and 18.00 °C, respectively.

The PXRD pattern of crystal harvested from metastable curve at different temperature were also overlaying to pure API pattern confirming the recrystallization of Metformin HCl. DSC thermogram showed melting of pure MET and crystals from metastable curve at 227.80 and 227.72 °C, respectively. TGA for material showed no solvent loss, only degradation temperature point was seen. Particle density of crystal nucleated at 65 and 55 °C was 1.362 ± 0.002 and 1.361 ± 0.002 g/cc, respectively.

Tableting properties were studied at molecular and macroscopic level. At the molecular level, crystal planes of 55 °C showed less compressible compared to crystal planes of 65 °C. All three planes of 65 °C have less Young's moduli compare to 55 °C, which indicates more spacing in planes of 65 °C. At the macroscopic level, crystal at 65 °C showed low YPpl and YPel compared to crystal at 55 °C. Elastic recovery was higher at 65 °C compared to 55 °C crystals. This resulted in greater compressibility of crystal at 55 °C. There was no statistically significant difference in work related parameters.

References

[1] H. Chen, A. Aburub, and C. C. Sun, “Direct Compression Tablet Containing 99% Active Ingredient—A Tale of Spherical Crystallization,” *Journal of Pharmaceutical Sciences*, 2019, doi: 10.1016/j.xphs.2018.11.015.

[2] T. S. Lumpe and T. Stankovic, “Exploring the property space of periodic cellular structures based on crystal networks,” *Proc Natl Acad Sci U S A*, 2021, doi: 10.1073/pnas.2003504118.

[3] P. Hartman and P. Bennema, “The attachment energy as a habit controlling factor. I. Theoretical considerations,” *Journal of Crystal Growth*, 1980, doi: 10.1016/0022-0248(80)90075-5.

[4] P. Barrett and B. Glennon, “Characterizing the metastable zone width and solubility curve using lasentec FBRM and PVM,” *Chemical Engineering Research and Design*, 2002, doi: 10.1205/026387602320776876.

[5] M. Takasuga and H. Ooshima, “Control of crystal size during oiling out crystallization of an API,” *Crystal Growth and Design*, 2014, doi: 10.1021/cg5011874.

[6] A. di Pretoro and F. Manenti, “Crystallization,” in *SpringerBriefs in Applied Sciences and Technology*, 2020. doi: 10.1007/978-3-030-34572-3_13.

[7] M. Pollak, “Metformin and other biguanides in oncology: Advancing the research agenda,” *Cancer Prevention Research*. 2010. doi: 10.1158/1940-6207.CAPR-10-0175.

[8] A. A. Baig *et al.*, “Effect of carbonate content and crystallinity on the metastable equilibrium solubility behavior of carbonated apatites,” *Journal of Colloid and Interface Science*, 1996, doi: 10.1006/jcis.1996.0255.

[9] D. J. W. Grant, M. Mehdizadeh, A. H. L. Chow, and J. E. Fairbrother, “Non-linear van’t Hoff solubility-temperature plots and their pharmaceutical interpretation,” *International Journal of Pharmaceutics*, 1984, doi: 10.1016/0378-5173(84)90104-2.

[10] R. v. Haware *et al.*, “Anisotropic crystal deformation measurements determined using powder X-ray diffraction and a new in situ compression stage,” *International Journal of Pharmaceutics*, 2011, doi: 10.1016/j.ijpharm.2011.06.021.

[11] S. Datta and D. J. W. Grant, “Crystal structures of drugs: Advances in determination, prediction and engineering,” *Nature Reviews Drug Discovery*. 2004. doi: 10.1038/nrd1280.

[12] P. Marchetti and R. Navalesi, “Pharmacokinetic-Pharmacodynamic Relationships of Oral Hypoglycaemic Agents: An Update,” *Clinical Pharmacokinetics*. 1989. doi: 10.2165/00003088-198916020-00004.

[13] J. D. Lalau, M. L. Azzoug, F. Kajbaf, C. Briet, and R. Desailloud, “Metformin accumulation without hyperlactataemia and metformin-induced hyperlactataemia without metformin accumulation,” *Diabetes and Metabolism*, 2014, doi: 10.1016/j.diabet.2013.12.003.

[14] G. A. Shabir, “Validation of high-performance liquid chromatography methods for pharmaceutical analysis: Understanding the differences and similarities between validation requirements of the US Food and Drug Administration, the US Pharmacopeia and the International Conf,” 2003. doi: 10.1016/S0021-9673(02)01536-4.

[15] FDA, “Guidance for Industry Analytical Procedures and Methods Validation,” *Federal Register*. 2000.

[16] International Council for Harmonisation (ICH), “ICH- Q2(R1),” 2005.

[17] A. Laird, A. Laird, M. Chougule, M. Hamad, and K. R. Morris, “Thermodynamics associated with monitoring pre-nucleation aggregation at high supersaturation,” *International Journal of Pharmaceutical Sciences Review and Research*, 2013.

[18] E. C. Lima, A. A. Gomes, and H. N. Tran, “Comparison of the nonlinear and linear forms of the van’t Hoff equation for calculation of adsorption thermodynamic parameters (ΔS° and ΔH°),” *Journal of Molecular Liquids*, 2020, doi: 10.1016/j.molliq.2020.113315.

[19] M. Paskevicius, D. A. Sheppard, and C. E. Buckley, “Thermodynamic changes in mechanochemically synthesized magnesium hydride nanoparticles,” *J Am Chem Soc*, 2010, doi: 10.1021/ja908398u.

[20] M. Fujiwara, P. S. Chow, D. L. Ma, and R. D. Braatz, “Paracetamol Crystallization Using Laser Backscattering and ATR-FTIR Spectroscopy: Metastability, Agglomeration, and Control,” *Crystal Growth and Design*, 2002, doi: 10.1021/cg0200098.

[21] C. Bian, H. Chen, X. Song, and J. Yu, “Metastable zone width and the primary nucleation kinetics for cooling crystallization of NaNO3 from NaCl-NaNO3-H2O system,” *Journal of Crystal Growth*, 2019, doi: 10.1016/j.jcrysgro.2019.04.013.

[22] S. L. Childs, L. J. Chyall, J. T. Dunlap, D. A. Coates, B. C. Stahly, and G. P. Stahly, "A metastable polymorph of metformin hydrochloride: Isolation and characterization using capillary crystallization and thermal microscopy techniques," *Crystal Growth and Design*, 2004, doi: 10.1021/cg034243p.

[23] W. Hemminger, "Thermal analysis: Fundamentals and applications to polymer science," *Thermochimica Acta*, 1995, doi: 10.1016/0040-6031(95)91503-6.

[24] R. L. Danley, "New modulated DSC measurement technique," *Thermochimica Acta*, 2003, doi: 10.1016/s0040-6031(02)00541-5.

[25] T. Instrument, "Modulated DSC® Paper# 2 Modulated DSC® Basics; Calculation and Calibration of MDSC® Signals," *Tainstruments.Co.Jp*, 2005.

[26] M. Saunders, "Thermal Analysis of Pharmaceuticals," in *Principles and Applications of Thermal Analysis*, 2008. doi: 10.1002/9780470697702.ch8.

[27] A. Jain, H. S. Shah, P. R. Johnson, A. S. Narang, K. R. Morris, and R. v. Haware, "Crystal anisotropy explains structure-mechanics impact on tableting performance of flufenamic acid polymorphs," *European Journal of Pharmaceutics and Biopharmaceutics*, 2018, doi: 10.1016/j.ejpb.2018.09.006.

[28] N. K. Thakral, R. L. Zanon, R. C. Kelly, and S. Thakral, "Applications of Powder X-Ray Diffraction in Small Molecule Pharmaceuticals: Achievements and Aspirations," *Journal of Pharmaceutical Sciences*. 2018. doi: 10.1016/j.xphs.2018.08.010.

[29] "The reflection of X-rays by crystals," *Proceedings of the Royal Society of London. Series A, Containing Papers of a Mathematical and Physical Character*, 1913, doi: 10.1098/rspa.1913.0040.

[30] H. Eren, "Density measurement," in *Measurement, Instrumentation, and Sensors Handbook: Spatial, Mechanical, Thermal, and Radiation Measurement, Second Edition*, 2017. doi: 10.1201/b15474.

[31] R. W. Heckel, "Density-Pressure Relationships in Powder Compaction," *Transactions of the Metallurgical Society of AIME*, 1961.

[32] R. v. Haware, I. Tho, and A. Bauer-Brandl, “Application of multivariate methods to compression behavior evaluation of directly compressible materials,” *European Journal of Pharmaceutics and Biopharmaceutics*, 2009, doi: 10.1016/j.ejpb.2008.11.008.

[33] G. Ragnarsson, “Force- Displacement and Network Measurements,” 1995. doi: 10.1201/b14207-5.

[34] United States Pharmacopoeia, “<1217> Tablet Breaking Force,” *Usp35-Nf30*, 2012.

[35] “Industrial crystallization process control,” *IEEE Control Systems*, 2006, doi: 10.1109/mcs.2006.1657878.

[36] R. R. Vippagunta, R. LoBrutto, C. K. Pan, and J. P. Lakshman, “Investigation of Metformin HCl lot-to-lot variation on flowability differences exhibited during drug product processing,” *Journal of Pharmaceutical Sciences*, 2010, doi: 10.1002/jps.22207.

[37] J. A. Bhatt, D. Bahl, K. Morris, L. L. Stevens, and R. v. Haware, “Structure-mechanics and improved tableting performance of the drug-drug cocrystal metformin:salicylic acid,” *European Journal of Pharmaceutics and Biopharmaceutics*, 2020, doi: 10.1016/j.ejpb.2020.05.031.